NUCL SCI TECH (2017) 28:145
DOI 10.1007/s41365-017-0299-3

An active base designed in high-counting-rate applications for Hamamatsu R1924A photomultiplier tube

Pei-Pei Ren[1,2] · Wei-Ping Lin[1] · Roy Wada[3] · Xing-Quan Liu[1] · Mei-Rong Huang[4] · Guo-Yu Tian[1,2] · Fei Luo[1,5] · Qi Sun[1,2] · Zhi-Qiang Chen[1] · Guo-Qing Xiao[1] · Rui Han[1] · Fu-Dong Shi[1] · Bo-Xing Gou[1]

Received: 20 March 2017 / Revised: 15 May 2017 / Accepted: 2 June 2017 / Published online: 6 September 2017

Abstract Hamamatsu R1924A is one of the most widely used photomultiplier tubes (PMTs) in nuclear physics. Since the active base suitable for R1924A is still not available in market, an active base is designed for Hamamatsu R1924A PMT, and the test results at high counting rates are presented. The active bases with two different sets of resistor chains were tested and compared by a frequency-controlled green straw hat LED light. A stable signal output up to 100 kHz is achieved using frequency-controlled LED pulsed light. The temperature of bases, which reflects the power consumption and is crucial for applications in vacuum, is also monitored with the same LED pulsed light. The temperature of the active base with smaller resistances reaches about twice of that of the active base with larger resistances in the resistor chain. For the applications in vacuum, the active base with resistance between the two sets of resistor chains may be preferable.

Keywords Active base · High counting rate · Hamamatsu R1924A photomultiplier tube

1 Introduction

For the centrality CsI array, described in Ref. [1], which is going to be used in experiments at the IMP, active bases have been studied. In the array, Hamamatsu R1924A tubes are used. R1924A is a small (25 mm in diameter) photomultiplier tube (PMT), which is a relatively fast (1.5-ns rising time) tube with a linear-focused 10-stage dynode geometry. The borosilicate entrance window gives a spectral response of wavelength, λ, from 300 to 650 nm with the peak at 420 nm. The photocathode is Bialkali with a 22% quantum efficiency at $\lambda = 420$ nm.

R1924A is one of the most widely used PMTs in nuclear physics. It has been applied to NIMROD-ISiS [2], the CCDA project [1] in IMP, an array to classify the centrality of heavy ion collisions, the Super-TIGER project [3], the Compton gamma imager [4], the GSO detector [5], the active veto system at LBNL low-background facility [6], our previous experiment [7–9], and so on. In most applications, the PMT has been conventionally operated with passive resistor bases, which consist of resistors and

This work was supported by the National Natural Science Foundation of China (Nos. 91426301 and 11075189), the Strategic Priority Research Program of the Chinese Academy of Sciences "ADS project" (No. XDA03030200), the Program for the CAS "Light of West China" (No. 29Y601030), and the US Department of Energy (No. DE–FG02–93ER40773). The authors also thank the program of the "visiting professorship of senior international scientists of the Chinese Academy of Sciences" for their support during his stay at the IMP.

✉ Wei-Ping Lin
linwp1204@impcas.ac.cn

Roy Wada
wada@comp.tamu.edu

[1] Institute of Modern Physics, Chinese Academy of Sciences, Lanzhou 730000, China

[2] University of Chinese Academy of Sciences, Beijing 100049, China

[3] Cyclotron Institute, Texas A&M University, College Station, TX 77843, USA

[4] College of Physics and Electronics information, Inner Mongolia University for Nationalities, Tongliao 028000, China

[5] University of Science and Technology of China, Hefei 230026, China

capacitors, to supply the dynode bias voltages at relatively low counting rate cases, just because of their simplicity. However, in most of the trigger detectors, such as a beam monitor counter or a centrality detector, the tube has to be operated in a high counting rate with large output pulses.

When the counting rate becomes high, i.e., more than 1 kHz, with pulse height larger than 1 V, the linear response between the light input and the output signal height does not hold and the output signals are reduced. This is called the "pulse height defect." The higher the frequency and the larger the output signal, the more the pulse height defect. The linear response is crucial for particle identification and energy measurement. The energy measurement is very important in applications not only for calorimetry [10], but also for the particle identifications, such as the $\Delta E - E$ method [2] and pulse shape discrimination [1]. In high counting rate, with large output signals, a large current is generated at the last dynode stages, which is supplied through the resistor chain and capacitors. This large current reduces the voltage between the last few dynodes and causes the pulse height defect. Field-effect transistors (FETs) [11] are capable for fast switching operations by a gate signal with relatively small heat generation and can provide high withstand voltage between the source and drain, which leads to a large drain current (ID) when the gate is opened. Taking advantage of the FET, the output signal stability would be improved by replacing the resistors with FETs in a passive base. This stabilized base is called an "active base." Therefore, the active base is a better choice in high-counting-rate applications.

This article is organized as follows: The active base designing and tests are presented in Sect. 2. The applications of the active base in high counting rate and in vacuum are discussed in Sect. 3. A brief summary is given in Sect. 4.

2 Designing and testing of active bases

To make an active base that is suitable for the R1924A tube and has a small length, four of STP2NK100Z FET, which is a n-channel MOSFET and has 1000 V withstand voltage, are used in the last four stages of the voltage supply. Figure 1 shows a schematic circuit diagram of the active base designed [12]. The four 15 MΩ and one 100 MΩ resistor chain in Fig. 1 distributes the bias voltages for FETs (dynode 7 to 10), and the other dynodes 1–6 are biased by $R1$, $R2$, and $R3$ resistor chains, respectively. The capacitors are used in the circuit to increase the stability of PMT output [13]. Two sets of resistor chains, which differ in 10 times resistance as shown in the bottom of Fig. 1, are used for the active base. We call them "base 1"(set1) and "base 2"(set2) throughout the paper.

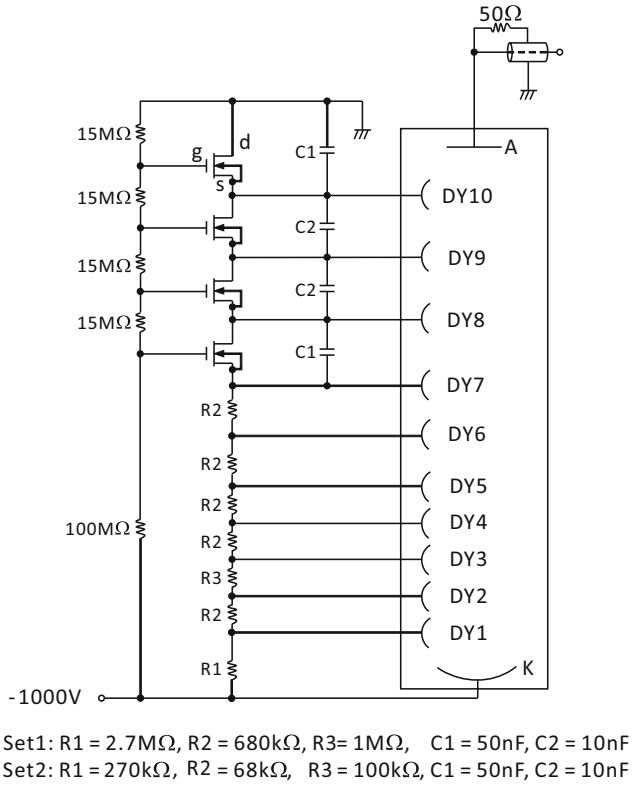

Fig. 1 PMT base circuit for R1924A tube. Two different sets of resistor chains are shown under the circuit

A 3-mm green straw hat LED, which wavelength is inside the PMT's spectral response, driven by the frequency-controlled circuit shown in Fig. 2, is used to test the newly designed active bases. A fast analog signal with less than 1 ns rise time is generated by a computer-controlled emulator (CAEN Mod. NDT68000). After discriminating by a constant fraction discriminator (ORTEC EG&G CF8000), a 140-ns gate signal from a gate and delay generator (ORTEC GG8020) is proceeded to the green LED. The photoelectrons generated by the light from the LED

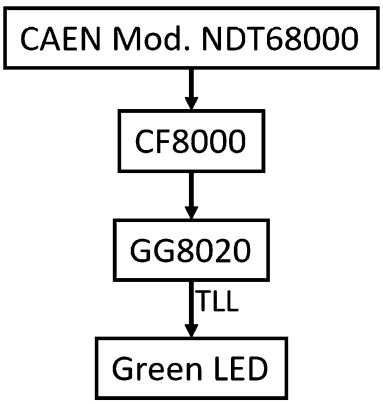

Fig. 2 The frequency-controlled circuit for green straw hat LED pulsed light

are collected and multiplied by the R1924A PMT inside a black box. The oscilloscope is used to read the output signal. To make a comparison, the passive base from Hamamatsu E2924 is also used as a reference. The same R1924A tube is used for all the three bases in the tests. Figure 3 shows the signal of PMT output recorded by the oscilloscope for passive base (blue line), base 1 (brown line), and base 2 (black line) at the LED pulsed light frequency of 0.1 kHz (a) and 50 kHz (b). The voltages are slightly adjusted, around −1000 V, to get the same peak value of 6 V as shown in Fig. 3a. One can see that the passive base shows notable oscillation in the peak, while base 1 is slightly better and base 2 is the best in signal shape at 0.1 kHz LED pulsed light. In Fig. 3b, the signal shapes are shown at 50 kHz. One can see clearly the pulse height defect for the passive base and base 1. In the following sections, more details of the pulse height defects as a function of the frequency are investigated.

To see the stability of signal output of three bases, we change the LED pulsed light frequency from 0.1 kHz to more than 100 kHz. The output signal for each frequency of LED light is recorded by the oscilloscope. The average value from the signal peak is assigned as the amplitude, which has less than 0.5 V uncertainty. The measured amplitude as a function of LED frequency is shown in Fig. 4 for passive base (open circles), base 1 (open squares), and base 2 (open triangles). The amplitude of passive base starts to drop after a LED frequency greater than 1 kHz and decreases monotonously as the LED frequency increases. The stability of the output signal for the two active bases is significantly extended. As one can see, the amplitude stays the same up to 10 kHz for base 1 and up to 100 kHz for base 2. A slightly increasing trend is observed for base 1 after 5 kHz. This could be from the signal oscillation at the peak mentioned above, which causes some errors to determine the amplitude. There is a minimum value before the amplitude drops monotonously for both two active bases, which could be caused by the ringing in the output signal [13].

Another important characteristic for PMT bases is the power consumption, which is crucial in vacuum applications. The more power is consumed, the more heat is generated by the base. One can get the relative power consumption by monitoring the temperature of the PMT bases. An apuhua TM-902C thermometer with an accuracy of 0.1°C is used to record the temperature of the bases in the tests. The temperature sensor is attached to the last stage of FETs for the active bases and to outer cover for the passive base, respectively. The same 1-kHz frequency pulsed LED light is used for this test. To remove the slight difference of room temperature, the ratio between base temperature and room temperature is used in the measurements. Figure 5 shows the temperature ratio, T/T_0 (T_0 is the room temperature), as a function of monitored time for passive base (solid line), base 1 (dotted line), and base 2 (dashed line). The base 1 with FETs and with $R1 = 2.7\,\mathrm{M\Omega}$, $R2 = 680\,\mathrm{k\Omega}$, and $R3 = 1\,\mathrm{M\Omega}$ shows the minimum power consumption and that the passive base comes at the second place, while base 2, with 10 times less the $R1$, $R2$, and $R3$ resistances comparing to that of base 1, shows the maximum power consumption.

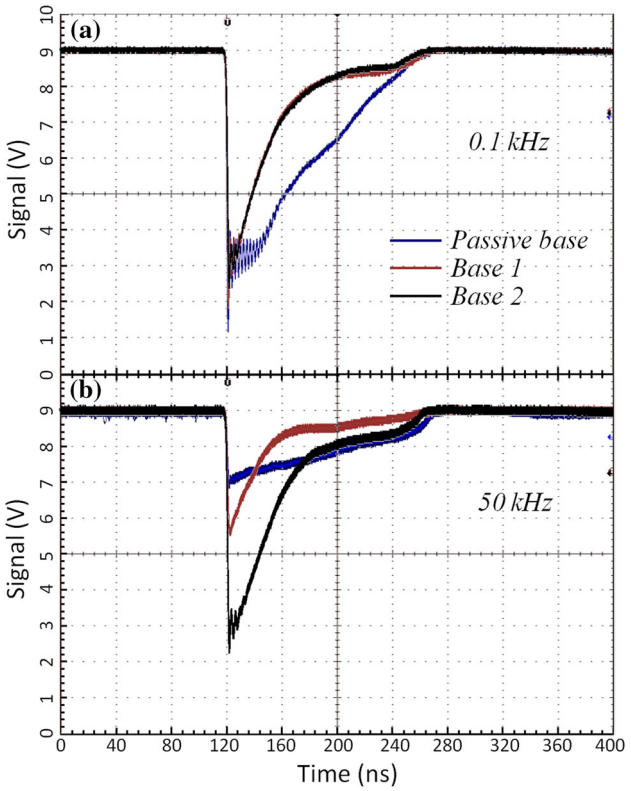

Fig. 3 (Color online) The signals of PMT output in the oscilloscope for the LED light frequency of 0.1 kHz (**a**) and 50 kHz (**b**). The *blue*, *brown*, and *black lines* correspond to passive base, base 1, and base 2, respectively

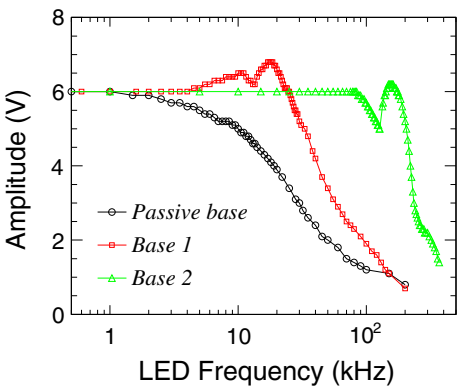

Fig. 4 (Color online) The pulse amplitude as a function of LED light frequency for passive base (*open circles*), base 1 (*open squares*), and base 2 (*open triangles*)

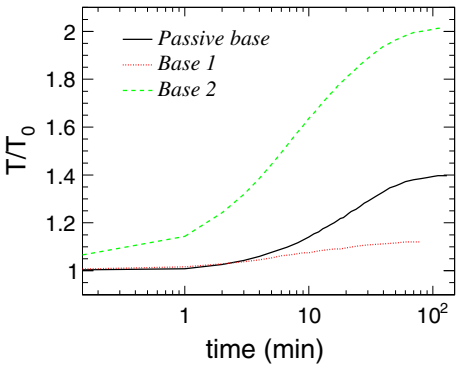

Fig. 5 (Color online) The base temperature (T) relative to the room temperature (T_0) as a function of monitoring time for passive base (*solid line*), base 1 (*dotted line*), and base 2 (*dashed line*) with 1 kHz LED light frequency

3 Discussion

From the results of frequency tests shown in Fig. 4, we conclude that the newly designed active bases (base 1 and 2) indeed extend the stability of R1924A PMT output signal to high frequencies, 10 kHz for base 1 and 100 kHz for base 2. The extension of the stability of output signal depends significantly on the resistances of $R1$, $R2$, and $R3$. The smaller the resistances, the more extension of stability in the output signal. On the other hand, the results of power consumption tests as shown in Fig. 5 reveal that the base with smaller resistance, i.e., base 2, has a much larger power consumption than that of larger resistances. This limits further reduction of the resistor values from those of base 2 to obtain the better stability for higher frequencies without extra cooling of the base.

All resistors are temperature dependent, which depends on their characteristics, and heat causes some instability, for either passive or active base application, especially for the first few hours after the voltage is turned on. Therefore, one needs to balance the stability in the high counting rate and the power consumption to get the best resistance set for $R1$, $R2$, and $R3$ in actual applications. For the applications in vacuum, the active base with resistance between the two sets of the resister chains, set 1 and set 2, may be preferable.

4 Summary

Hamamatsu R1924A is one of the most widely used PMTs in nuclear physics. An active base with FETs on the last four stages, which is still not available in market for Hamamatsu R1924A PMT, is designed and tested for high-counting-rate application. The active bases with two sets of the resistor chains were tested. A straw hat LED pulsed light, driven by a frequency-controlled circuit, was used in the stability of output signal and power consumption tests. A stable output signal with 6 V in the amplitude up to the LED pulsed light frequency of 100 kHz is achieved for the base with smaller resistances in resistor chain. In the power consumption tests, the temperature for the active base with smaller resistances reaches about twice of that of the active base with larger resistances in resistor chain, which limits the further reduction of resistances of $R1$ to $R3$ for extending the stability of output signal to a higher counting rate. For the applications in a vacuum, the active base with resistance between the two sets of the resister chains may be preferable.

References

1. F. Fu, W.P. Lin, X.Q. Liu et al., A module test of CCDA: an array to select the centrality of collisions in heavy ion collisions. Chin. Phys. Lett. **31**, 082502 (2014). doi:10.1088/0256-307X/31/8/082502
2. S. Wuenschel, K. Hagel, R. Wada et al., NIMROD-ISiS, a versatile tool for studying the isotopic degree of freedom in heavy ion collisions. Nucl. Instrum. Methods Phys. Res. A **604**, 578 (2009). doi:10.1016/j.nima.2009.03.187
3. M. Sasaki, W. R. Binns, R. G. Bose et al., Super-TIGER 2012/2013 in-flight instrument performance and preliminary results. International Cosmic Ray Conference, 0570 (2013). http://galprop.stanford.edu/elibrary/icrc/2013/papers/icrc2013-0570.pdf
4. P.R.B. Saull, L.E. Sinclair, H.C.J. Seywerd et al., First demonstration of a Compton gamma imager based on silicon photomultipliers. Nucl. Instrum. Methods Phys. Res. A **679**, 89 (2012). doi:10.1016/j.nima.2012.03.019
5. S. Yamamoto, Optimization of the integration time of pulse shape analysis for dual-layer GSO detector with different amount of Ce. Nucl. Instrum. Methods Phys. Res. A **587**, 319–323 (2008). doi:10.1016/j.nima.2008.01.084
6. K.J. Thomas, E.B. Norman, A.R. Smith et al., Installation of a muon veto for low background gamma spectroscopy at the LBNL low-background facility. Nucl. Instrum. Methods Phys. Res. A **724**, 47–53 (2013). doi:10.1016/j.nima.2013.05.034
7. M. Huang, Z. Chen, S. Kowalski et al., Isobaric yield ratios and the symmetry energy in heavy-ion reactions near the Fermi energy. Phys. Rev. C **81**, 044620 (2010). doi:10.1103/PhysRevC.81.044620
8. M.R.D. Rodrigues, W. Lin, X. Liu et al., Experimental reconstruction of excitation energies of primary hot isotopes in heavy ion collisions near the Fermi energy. Phys. Rev. C **88**, 034605 (2013). doi:10.1103/PhysRevC.88.034605
9. R. Wada, M.R. Huang, W.P. Lin et al., IMF production and symmetry energy in heavy ion collisions near Fermi energy. Nucl. Sci. Technol. **24**, 050501 (2013). doi:10.13538/j.1001-8042/nst.2013.05.001
10. S.S. Gao, C.Q. Feng, D. Jiang et al., Radiation tolerance studies on the VA32 ASIC for DAMPE BGO calorimeter. Nucl. Sci. Technol. **25**, 010402 (2014). doi:10.13538/j.1001-8042/nst.25.010402
11. Feild-effect transistor, wiki, https://en.wikipedia.org/wiki/Field-effect_transistor

12. S. Takeuchi, T. Nagai, Low power photomultiplier base circuit. IEEE Trans. Nucl. Sci. **32**, 78 (1985). doi:10.1109/TNS.1985.4336794

13. Hamamatsu Photonics, "Chapter 5: How to use photomultiplier tubs and peripheral circuits." (2007). www.hamamatsu.com/resources/pdf/etd/PMT_handbook_v3aE-Chapter5.pdf